The EMBO Journal (2009) 28, 3329–3340 | © 2009 European Molecular Biology Organization | All Rights Reserved 0261-4189/09
www.embojournal.org

THE EMBO JOURNAL

The kinase TNIK is an essential activator of Wnt target genes

Tokameh Mahmoudi[1,4], Vivian SW Li[1,4], Ser Sue Ng[1], Nadia Taouatas[2,3], Robert GJ Vries[1], Shabaz Mohammed[2,3], Albert J Heck[2,3] and Hans Clevers[1,*]

[1]Hubrecht Institute—KNAW and University Medical Centre Utrecht, Utrecht, The Netherlands, [2]Biomolecular Mass Spectrometry and Proteomics Group, Bijvoet Center for Biomolecular Research and Utrecht Institute for Pharmaceutical Sciences, Utrecht University, Utrecht, The Netherlands and [3]Netherlands Proteomics Centre, Utrecht, The Netherlands

Wnt signalling maintains the undifferentiated state of intestinal crypt/progenitor cells through the TCF4/β-catenin-activating transcriptional complex. In colorectal cancer, activating mutations in Wnt pathway components lead to inappropriate activation of the TCF4/β-catenin transcriptional programme and tumourigenesis. The mechanisms by which TCF4/β-catenin activate key target genes are not well understood. Using a proteomics approach, we identified Tnik, a member of the germinal centre kinase family as a Tcf4 interactor in the proliferative crypts of mouse small intestine. Tnik is recruited to promoters of Wnt target genes in mouse crypts and in Ls174T colorectal cancer cells in a β-catenin-dependent manner. Depletion of TNIK and expression of TNIK kinase mutants abrogated TCF–LEF transcription, highlighting the essential function of the kinase activity in Wnt target gene activation. *In vitro* binding and kinase assays show that TNIK directly binds both TCF4 and β-catenin and phosphorylates TCF4. siRNA depletion of TNIK followed by expression array analysis showed that TNIK is an essential, specific activator of Wnt transcriptional programme. This kinase may present an attractive candidate for drug targeting in colorectal cancer.

The EMBO Journal (2009) **28,** 3329–3340. doi:10.1038/emboj.2009.285; Published online 8 October 2009
Subject Categories: signal transduction; chromatin & transcription
Keywords: β-catenin; TCF4; TNIK; Wnt

Introduction

When Wnt signals engage their receptors, a complex series of biochemical events is set in motion, leading to stabilization of the key signalling molecule β-catenin in the cytoplasm. On transfer to the nucleus, stabilized β-catenin forms a complex with DNA-binding TCF/LEF transcription factors and serves as a transcriptional co-activator, thus switching on Wnt target genes (Behrens *et al*, 1996; Molenaar *et al*, 1996). A primary function of canonical Wnt signalling in adult mammals involves the maintenance of stem and progenitor cells in the intestinal epithelium (Clevers, 2006).

Mutational activation of the TCF4/β-catenin transcriptional programme can lead to various types of cancer, most notably of the intestine. In these tumours, loss of the Wnt pathway inhibitors APC and Axin2 (Rubinfeld *et al*, 1996; Liu *et al*, 2000) or activating point mutations in β-catenin (Korinek *et al*, 1997; Morin *et al*, 1997) lead to the stabilization of β-catenin. The constitutive presence of TCF4/β-catenin complexes locks the Wnt transcriptional programme in the 'on' state (Korinek *et al*, 1998; Bienz and Clevers, 2000), leading to transformation in the gut epithelium. At present, the mechanisms by which the β-catenin/TCF4 complex activates expression of key target genes are incompletely understood. Functions have been proposed for a number of co-activators including CBP/p300 (Hecht *et al*, 2000; Takemaru and Moon, 2000), Brg1 (Barker *et al*, 2001) and Pygopus/Bcl9 complexes (Kramps *et al*, 2002; Mosimann *et al*, 2009). Identification of the complete repertoire of nuclear TCF4/β-catenin co-activator complex components will be critical as potential drug targets to inhibit the aberrantly activated Wnt transcriptional programme in colorectal cancer.

In this study, using a proteomics approach, we identified Traf2 and Nck-interacting kinase (Tnik) as a novel protein interacting with Tcf4 in the mouse intestinal crypt. Tnik is a member of germinal centre kinases (GCKs) possessing an N-terminal kinase domain and can specifically activate the c-Jun N-terminal kinase pathway similar to many GCKs (Fu *et al*, 1999). In addition, Tnik has also been reported as an effector of Rap2 to regulate actin cytoskeleton by disrupting F-actin structure, and subsequently inhibits cell spreading (Fu *et al*, 1999; Taira *et al*, 2004). However, a potential function for Tnik in transcriptional regulation has never been documented.

Here, we report that TNIK is a critical component of the transcriptional regulatory complex in the Wnt-signalling pathway. TNIK is localized in the nuclei of Wnt active intestinal crypts and is recruited to promoters of Wnt target genes in mouse crypts and in colorectal cancer cells in a β-catenin-dependent manner. TNIK interacts directly with both β-catenin and TCF4 and phosphorylates TCF4 leading to TCF/LEF-driven transcriptional activation of Wnt target genes. Exogenous expression of TNIK kinase mutants abrogate TCF/LEF-driven transcription, whereas siRNA depletion of TNIK followed by expression array analysis shows the critical function of TNIK as an essential and specific activator of Wnt target genes.

*Corresponding author. Netherlands Institute for Developmental Biology, Center for Biomedical Genetics, Hubrecht Institute for Developmental Biology and Stem Cell Research, University Medical Centre Utrecht, Uppsalalaan 8, 3584CT, Utrecht, The Netherlands. Tel.: +31 30 2121 826; Fax: +31 30 2121 801; E-mail: h.clevers@niob.knaw.nl
[4]These authors contributed equally to work

Received: 14 July 2009; accepted: 3 September 2009; published online: 8 October 2009

Results and discussion

Tnik co-immunoprecipitates with Tcf4 in the mouse small intestinal crypt

As an unbiased approach towards the identification of components of the endogenous TCF4 complex in murine small intestinal crypts and villi, we applied the combination of affinity purification and mass spectrometry (MS). We first developed a fractionation method to separate proliferative crypt epithelium from differentiated villus epithelium. The quality of the fractionation was assessed by western blot analysis of known proteins differentially expressed between the two compartments. The TCF4/β-catenin target genes/crypt markers c-Myc (He *et al*, 1998), EPHB2 and EPHB3 (van de Wetering *et al*, 2002) were strongly enriched in the crypt fraction, whereas the villus marker Keratin 20 (Calnek and Quaroni, 1993) was present exclusively in the purified villus fraction (Figure 1A). TCF4 was detected in both crypt and villus fractions, as was tubulin.

To identify potential Tcf4 co-regulators in a physiological *in vivo* setting, we immunopurified Tcf4 from crypt and villus fractions using a TCF4 antibody as well as a non-immune IgG as control. The immunoprecipitates were subjected to SDS–PAGE and silver staining (Figure 1B), followed by mass spectrometric identification. Tcf4 and β-catenin were readily identified in the crypt fraction, whereas Tcf4, but not β-catenin, was found in the villus fraction (Supplementary Figure S1A and B). None of these proteins were observed in the IgG control. This implied that the approach allowed us to specifically isolate Wnt-activated Tcf4 complexes from crypts and inactive Tcf4 from villi. Among the proteins specifically co-precipitating with Tcf4/β-catenin from the crypt fraction, the serine/threonine kinase Tnik stood out in that a large portion of the protein sequence was covered by the MS-identified peptides (Figure 1C; Supplementary Figure S1C). To confirm the interaction, we immunoprecipitated Tcf4 from crypt and villus fractions and probed for its association with endogenous Tnik by western blotting using a Tnik antibody. Despite the presence of Tnik protein in both fractions (Figure 1A), Tcf4 interacted with Tnik specifically in the crypt, but not the differentiated villus fraction (Figure 1D, top panels). Immunoprecipitation (IP) of β-catenin from crypts followed by western blot analysis also detected Tnik (Figure 1D, bottom left). The same endogenous interactions were confirmed in reverse, using the Tnik antibody for IP (Figure 1D, bottom right). These results showed that Tnik specifically interacts with the Tcf4/β-catenin complex in murine small intestinal crypts.

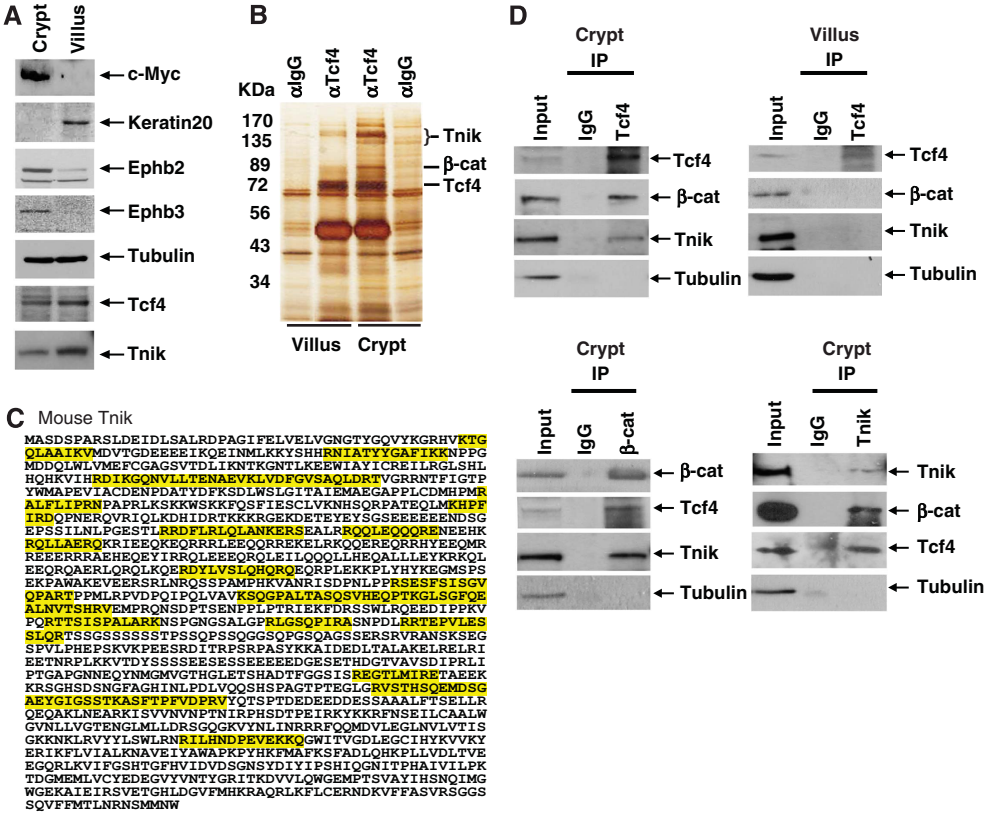

Figure 1 Tnik co-immunoprecipitates with Tcf4 in the mouse small intestinal crypt. (**A**) Biochemical purification of crypt and villus fractions from mouse small intestine used in Mass Spec experiment. Western blot analysis using antibodies directed against genes expressed specifically in the crypt (c-Myc, Ephb2 and Ephb3), villus (Keratin 20), as well as tubulin as control were used to assess the quality of the purified fractions. (**B**) Silverstained gel of Tcf4 containing complexes immunoprecipitated from purified crypt and villus fractions using antibody directed against Tcf4. The Tcf4-interacting proteins are indicated by arrows and were identified by MS (see Material and methods for details). (**C**) Peptide coverage of Tnik in MS experiment. Amino-acid sequences of Tnik peptides detected in the Tcf4 immunoprecipitate from crypt lysates are highlighted in yellow. (**D**) Cell lysates from purified crypt and villus fractions were immunoprecipitated with antibodies directed against endogenous Tcf4, β-catenin and Tnik as indicated and analysed by western blotting with the indicated antibodies.

Nuclear localization of Tnik in Wnt-activated intestinal crypt

Tnik has been earlier reported to localize in the cytoplasm and interact with and phosphorylate cytoskeletal structures (Fu *et al*, 1999). The presence of Tnik in the Tcf4 transcriptional complex suggested nuclear localization of Tnik. We next examined the expression of TNIK in mouse and human intestinal tissue using immunohistochemistry (IHC). Tnik was detected in both mouse small intestinal and colonic epithelia (Figure 2A–D). Nuclear localization of Tnik was detected specifically in Wnt-activated intestinal crypt (Figure 2B), consolidating our MS findings on the specific interaction of Tnik with Tcf4 in mouse intestinal crypt, but not villus. Using a mouse monoclonal antibody against the intermediate part of human TNIK, we further confirmed the nuclear localization of human TNIK in normal colonic epithelia as well as colorectal cancer tissues (Figure 2E–H). These results show that in addition to the reported cytoplasmic expression, Tnik is strongly enriched in the cell nuclei of Wnt-activated intestinal crypts.

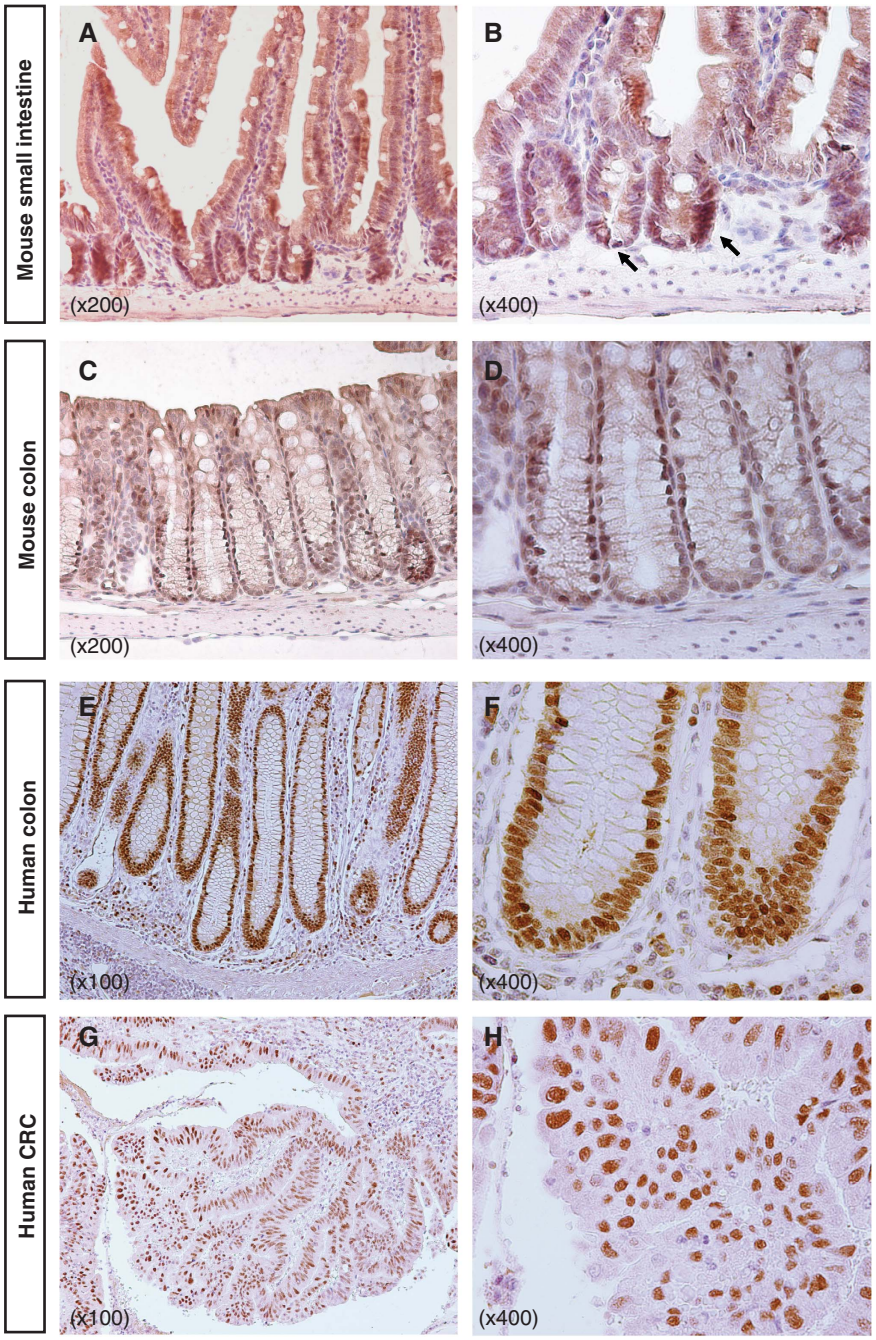

Figure 2 Nuclear localization of Tnik in Wnt-activated intestinal crypt. IHC of Tnik in mouse small intestine (**A**, **B**), mouse colon (**C**, **D**), human normal colon (**E**, **F**) and human colorectal tissues (**G**, **H**). (B) Nuclear localization of Tnik in mouse intestinal crypt is indicated by arrows. Corresponding magnification is shown on the bottom left of figures.

Tnik is recruited to the proximal promoters of Wnt target genes in mouse small intestinal crypts in vivo

We have earlier determined TCF4-binding sites by genome-wide chromatin IP (ChIP) in human colon cancer cells (Hatzis *et al*, 2008). To test whether Tnik is associated with such Tcf4/β-catenin response elements *in vivo,* we performed ChIP on purified intestinal crypt and villus fractions with antibodies specific for Tcf4, β-catenin and Tnik. Quantitative PCR (qPCR) analysis of the immunoprecipitated material was performed for homologous elements in two murine intestinal Wnt target genes, the Axin2 and c-Myc proximal promoters and up/downstream control regions (Figure 3A). As expected, Tcf4 was bound specifically to the target gene promoters in both the crypt and villus, whereas β-catenin was enriched on the target promoters specifically in the crypt-proliferative compartment (Figure 3A). Although not enriched on up/downstream control regions, Tnik was specifically recruited to the promoters of the two Wnt targets genes in the crypt, but not the villus fraction (Figure 3A).

TNIK is recruited to Wnt target genes in a β-catenin-dependent manner

To examine whether the Tcf4-Tnik association was mediated by β-catenin, we used a stable transfectant of the human

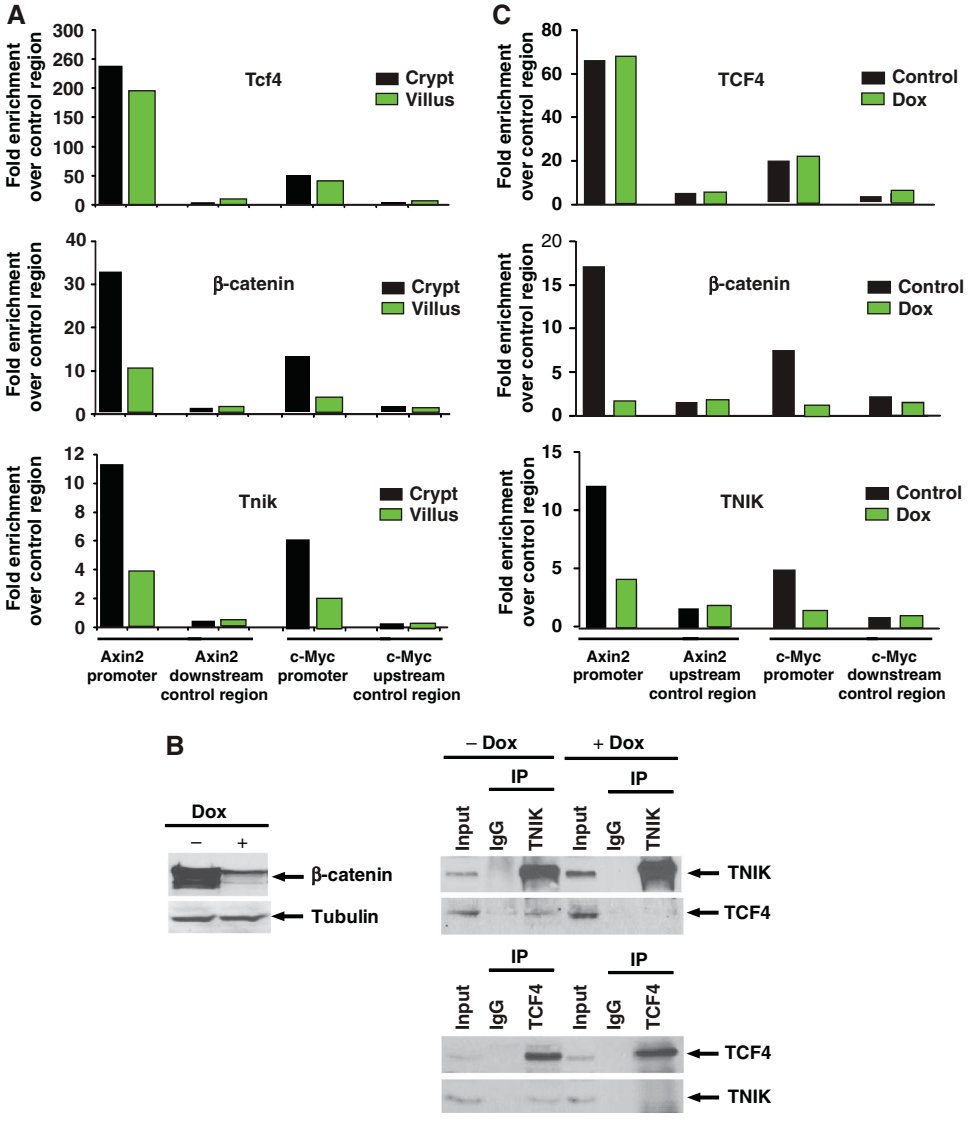

Figure 3 Tnik is recruited to Wnt target genes in mouse crypts and CRC cells in β-catenin-dependent manner. (**A**) Purified crypt and villus fractions from mouse small intestine were subjected to ChIP using antibodies directed against Tcf4, β-catenin and Tnik. Formaldehyde cross-linked chromatin was immunoprecipitated with the specified antibodies followed by qPCR using primers specific for the Axin2 and c-Myc proximal promoters as well as Axin2 downstream and c-Myc upstream control regions as indicated. The results are presented as relative enrichment over the non-bound downstream SP5 control region and are representative of three independent experiments. (**B**) TNIK interaction with TCF4 is mediated by β-catenin. Western blot analysis of β-catenin depletion in Ls174T cells expressing doxycycline (Dox) inducible β-catenin shRNA (left panel). Immunoprecipitated TNIK–protein complexes from untreated or doxycycline-treated cells were resolved by SDS–PAGE followed by western blotting using antibodies directed against TNIK and TCF4 (top right panel), and the result was further confirmed by the reverse IP (bottom right panel). (**C**) ChIP experiments in Ls174T cells uninduced or induced with Dox using antibodies specific for TCF4, β-catenin, and TNIK. The immunoprecipitated DNA was analysed by qPCR using primer pairs specific for the Axin2 and c-Myc promoters, and Axin2 upstream and c-Myc downstream control regions. The results are presented as relative enrichment over the non-bound second exon of the myoglobin gene and are representative of three independent experiments.

colon cancer cell line Ls174T, which expresses an shRNA targeting β-catenin in response to doxycycline treatment (van de Wetering *et al*, 2003). Of note, Ls174T cells harbour a stabilizing oncogenic mutation in β-catenin, resulting in the constitutive presence of β-catenin/TCF4 nuclear complexes. In the transfected cells, the β-catenin protein was strongly reduced 72 h post-doxycycline treatment (Figure 3B, left panel). We immunoprecipitated TNIK from the Ls174T cells with and without doxycycline treatment and probed for the presence of TCF4. TCF4 bound TNIK in these cells showing conservation of the TCF4–TNIK association across mammalian species (Figure 3B, right top panel). However, depletion of β-catenin resulted in loss of the TNIK/TCF4 interaction, implying that β-catenin serves as a bridge. Conversely, IP of TCF4 in β-catenin-depleted cells resulted in loss of TCF4–TNIK interaction (Figure 3B, bottom right panel). Using the same system, we examined the recruitment of TNIK to the promoters of TCF4 target genes Axin2 and c-Myc *in vivo* in the presence or absence of β-catenin (Figure 3C). TCF4 was bound to the Axin2 and c-Myc proximal promoters regardless of β-catenin status. As expected, β-catenin disappeared from the target gene promoters on β-catenin knockdown. Importantly, although specifically present on the Axin2 and c-Myc promoters, TNIK enrichment over these targets was decreased on β-catenin depletion (Figure 3C). Thus, TNIK recruitment to TCF4 target genes Axin2 and c-Myc occurs in a β-catenin-dependent manner.

The kinase activity of TNIK is required for TCF/LEF transcriptional activation

The specific association of TNIK with β-catenin/TCF4 in crypts and Ls174T cells was suggestive of a co-activator function for TNIK. To test this, we depleted TNIK from Ls174T cells using transient siRNA transfection and examined the effect on transcriptional activity of a Tcf-reporter TOPFlash (Figure 4A). Removal of TNIK by siRNA resulted in specific suppression of TOPFlash activity, but not of the mutant FOPFlash control. Similar suppression of TOPFlash activity was observed on TNIK depletion in another colorectal cancer cell line, SW480 (Supplementary Figure S2A). Conversely, over-expression of wild-type (WT) Flag-TNIK resulted in a dosage-dependent specific increase in TOPFlash activity (Figure 4C, right panel). The N-terminal kinase domain of TNIK is highly conserved among serine/threonine protein kinases (e.g. Ste20 family and protein kinase A) and contains several characterized subdomains that fold into a catalytic core structure (Hanks and Hunter, 1995) (Figure 4B). To examine the function of the kinase activity of TNIK in TCF/LEF-mediated transcriptional activation, we generated dominant negative TNIK kinase mutants TNIK R152A/D153A, TNIK K54A and TNIK D171A/F172A, harbouring mutations in the distinct conserved subdomains IV, II and VII respectively, essential to catalytic activity. Expression of increasing amounts of dominant negative TNIK kinase mutants in Ls174T colorectal cancer cells was examined by western blotting (Figure 4C, bottom panels). As earlier reported, WT TNIK migrates as two bands comprising phosphorylated and unphosphorylated forms (Figure 4C, right bottom) (Taira *et al*, 2004). All TNIK kinase mutants lacked the lower mobility phosphorylated form of WT TNIK, consistent with their inability to autophosphorylate. As shown in Figure 4C, expression of all TNIK kinase mutants abolished Tcf-reporter TOPFlash transcription activity in a dose-dependent manner. The results were further confirmed in another colorectal cancer cell line DLD1 (Supplementary Figure S2B). Thus, while depletion of TNIK by siRNA compromises TOPFlash activity, exogenous expression of kinase mutant TNIK results in a dominant negative effect, abrogating on TOPFlash-reporter activity.

We next tested whether TNIK can phosphorylate TCF4 or β-catenin using *in vitro* kinase assay. We immunoprecipitated WT or kinase mutant TNIK from 293T cells and performed *in vitro* kinase assays using GST–TCF4 and GST–β-catenin as substrate as shown in Figure 4D. As reported earlier, WT TNIK was capable of autophosphorylation (Fu *et al*, 1999), whereas the kinase mutants failed to autophosphorylate (Figure 4D). Importantly, WT TNIK, and not the kinase mutants, specifically phosphorylated GST–TCF4, identifying TCF4 as a substrate for TNIK kinase activity (Figure 4D). Taken together, these results show that the kinase activity of TNIK is essential to its function as a TCF4/β-catenin co-activator.

TNIK interacts directly with both TCF4 and β-catenin

To confirm the function of TNIK in regulation of the Wnt target gene expression, we used the HEK293T cell line in which the Wnt pathway is present, yet not mutationally activated. We examined the interaction between TNIK and TCF4 in HEK293T cells treated with either control or Wnt3A-conditioned media for 8 h. TNIK was immunoprecipitated from HEK293T lysates and probed for interaction with TCF4 and β-catenin by western blotting (Figure 5A, top panel). Although absent from the TNIK complex in the absence of Wnt signalling, both TCF4 and β-catenin specifically associated with TNIK in response to Wnt treatment. Conversely, IP of TCF4 from HEK293T lysates (either untreated or treated with Wnt) showed a Wnt-induced interaction with TNIK (Figure 5A, bottom panel). As expected, the interaction between β-catenin and TCF4 was Wnt dependent. Next, we examined the effect of siRNA-mediated knockdown of TNIK on TCF/β-catenin-mediated TOP/FOP transcriptional activation in the presence and absence of Wnt. Significant depletion of TNIK was accomplished at 72 h post siRNA treatment (Figure 5B, top panel). Removal of TNIK resulted in specific suppression of Wnt-dependent TOPFlash activity (Figure 5B, bottom panel). We concluded that TNIK is required for optimal TCF4/β-catenin transcriptional activation in response to Wnt.

We next probed whether TNIK can directly contact TCF4/β-catenin using *in vitro* binding assays. We generated *in vitro* translated radiolabelled TNIK deletion mutants (shown in Figure 5C) and probed their direct binding to GST-fused TCF4 and β-catenin immobilized on glutathione beads. The TNIK kinase domain and the kinase domain-containing ΔC bound TCF4 (Figure 5C middle panel), but not to control GST beads (Figure 5C, left panel), whereas the ΔK TNIK lacking the kinase domain was incapable of binding TCF4 (Figure 5C, middle panel). Thus, the TNIK kinase domain directly contacts TCF4. β-catenin also displayed direct binding to TNIK. The TNIK intermediate domain and deletion mutants ΔC and ΔK, which contain the intermediate region, bound β-catenin, pointing to this region of TNIK as the β-catenin interaction interface (Figure 5C, right panel). Thus, different domains of TNIK directly contact both TCF4 and β-catenin.

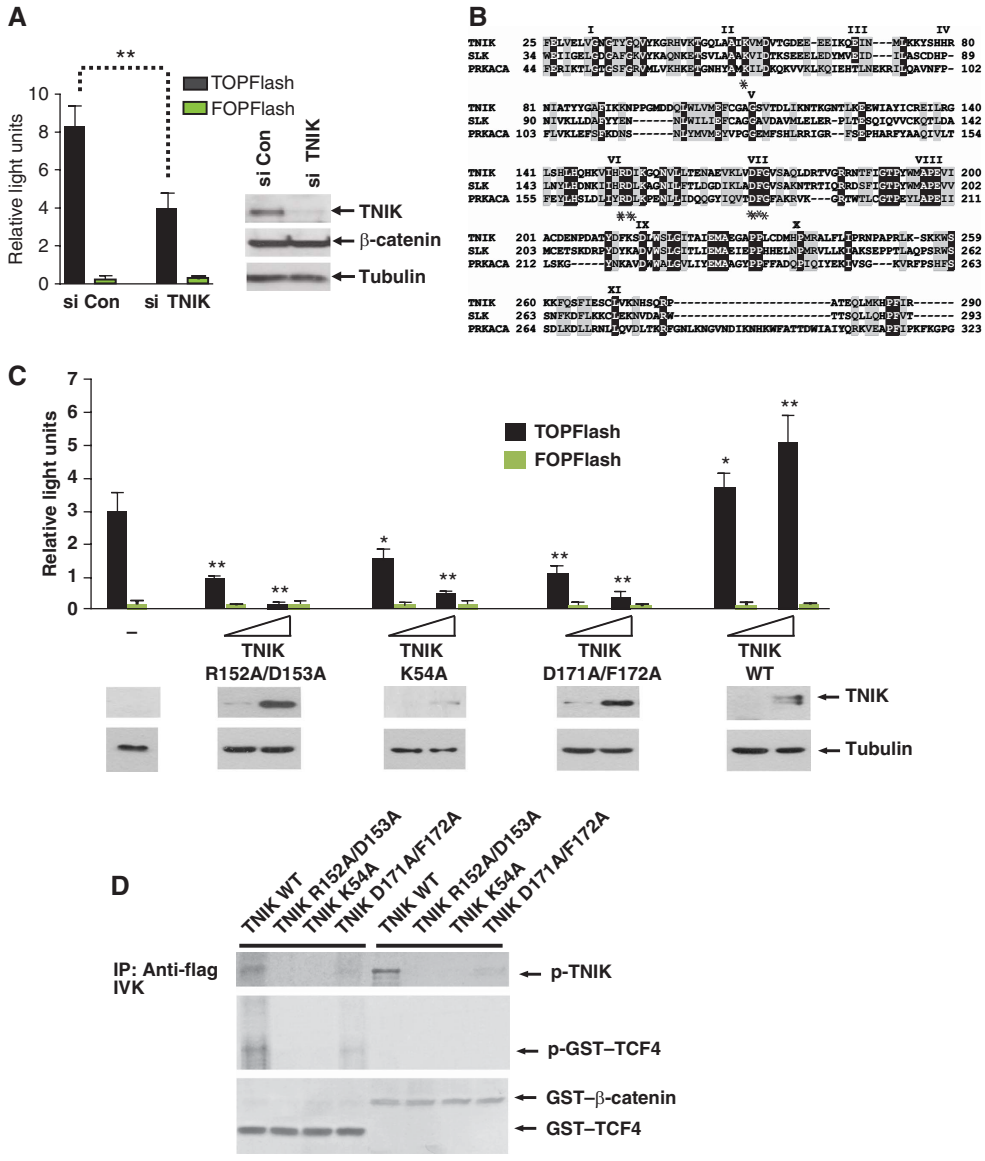

Figure 4 TNIK kinase activity is required for TCF/LEF-mediated transcription. (**A**) siRNA-mediated depletion of TNIK reduces β-catenin/TCF-driven transcription in Ls174T CRCs. Activity of the TOPFlash (black bars) and FOPFlash (green bars) 96 h post siRNA transfection is shown. Error bars represent standard deviation from three independent experiments. Expression of TNIK, β-catenin and control tubulin was analysed by western blotting after depletion of TNIK (left panel). (**B**) Amino-acid alignment of the N-terminal kinase domain of human TNIK with Ser/Thr kinases SLK and PRKACA. Identical amino acids are shown in black and conserved amino acids are highlighted in grey. Asterisks indicate the conserved amino acids mutated to generate TNIK mutants used in (C). (**C**) Expression of TNIK kinase mutants (second, third and fourth panels) abrogates β-catenin/TCF-driven transcription, whereas over expression of WT TNIK (last panel) specifically increases β-catenin/TCF-driven transcription in Ls174T CRCs. Black bars indicate TOPFlash activity, whereas green bars indicate FOPFlash activity 24 h post transfection of expression vectors. Error bars represent standard deviation from three independent experiments. Western blot analysis indicates expression of Flag-tagged WT and mutant TNIK proteins using M2 Flag antisera (bottom panel). **P*-value < 0.05, ***P*-value < 0.01. (**D**) Phosphorylation of TCF4 by TNIK is shown by *in vitro* kinase assay using immunoprecipitated Flag-tagged WT and mutant TNIK and GST–TCF4 and GST–β-catenin as substrate. WT TNIK is able to phosphorylate TCF4, but not β-catenin, whereas the phosphorylation is largely suppressed in all the TNIK kinase mutants. Autophosphorylation of WT TNIK is also detected. GST-tagged protein input is shown at the bottom.

TNIK is an essential and specific activator of Wnt target genes in HEK293T cells

To determine the function for TNIK in the control of endogenous Wnt target gene expression, we studied the effect of TNIK depletion in HEK293T cell line stimulated with Wnt3A by microarray analysis. We first characterized the Wnt target gene programme of HEK293T cells by inducing the cells with Wnt3A-conditioned medium followed by microarray expression analysis at three early time points, that is 4, 7 and 9 h. This resulted in 172 overlapping probes representing 144 unique genes (Figure 6A; Supplementary Table S1) selected against 1.5-fold increase at either 7 or 9 h time points of Wnt induction. Although some of the Wnt-induced genes were earlier described as Wnt target genes, such as TCF7 (Roose *et al*, 1999), CCND1 (Tetsu and McCormick, 1999) and AXIN2 (Yan *et al*, 2001; Jho *et al*, 2002; Lustig *et al*, 2002) in other cell/tissue types (http://www.stanford.edu/~rnusse/Wntwindow.html), the large majority were unique to the HEK293 kidney cells. These include various transcription factors such as BACH2, ID1, YY1, ETS2 and RUNX3. To

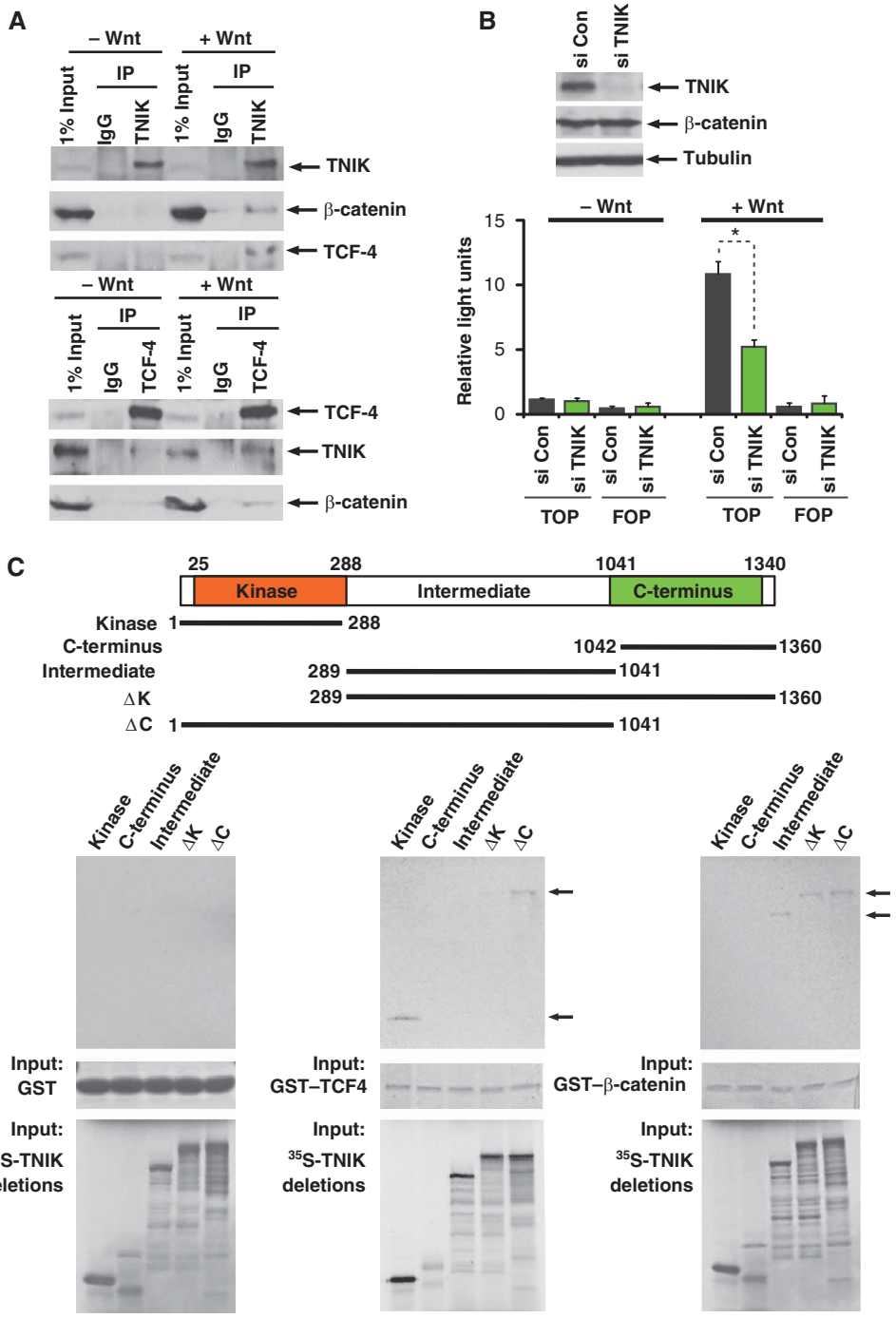

Figure 5 TNIK is interacting with TCF4 in β-catenin-dependent manner. (**A**) TNIK interacts with TCF4 and β-catenin on Wnt stimulation in HEK293T cells. Lysates from cells stimulated with either Wnt3A- or control-conditioned media as indicated for 8 h were used to immunoprecipitate TCF4 (bottom panel) or TNIK (top panel) and their associated proteins. Immunoprecipitated protein complexes were resolved by SDS–PAGE followed by western blotting using antibodies directed against TNIK, β-catenin and TCF4 as indicated. (**B**) siRNA-mediated depletion of TNIK reduces β-catenin/TCF-driven transcription in HEK293T cells. Expression of TNIK and control tubulin was analysed by western blotting after depletion of TNIK (top panel). Activity of the TOPFlash and FOPFlash 12 h post Wnt stimulation is shown (bottom panel). Error bars represent standard deviation from three independent experiments. **P*-value = 0.006. (**C**) Schematic summary of different TNIK deletion mutants (top panel). All five TNIK deletion mutants were *in vitro* translated with ^{35}S-labelled methionine and were incubated with GST–TCF4 or GST–β-catenin to examine the direct interaction. GST protein alone was used as control (bottom left panel). Only TNIK kinase and ΔC domains bind to GST–TCF4 (bottom middle panel, arrows), whereas TNIK intermediate, ΔK and ΔC domains bind to GST–β-catenin (bottom right panel, arrows).

increase the likelihood of examining direct transcriptional effects, we then focused on the 4 and 7 h time points to examine Wnt-induced expression profile changes on TNIK depletion.

By comparing the expression pattern of Wnt induction in TNIK-depleted cells to the Wnt-activated genes with >1.5-fold increase at 7 h Wnt induction, depletion of TNIK by siRNA resulted in a consistent opposite pattern in both 4 and

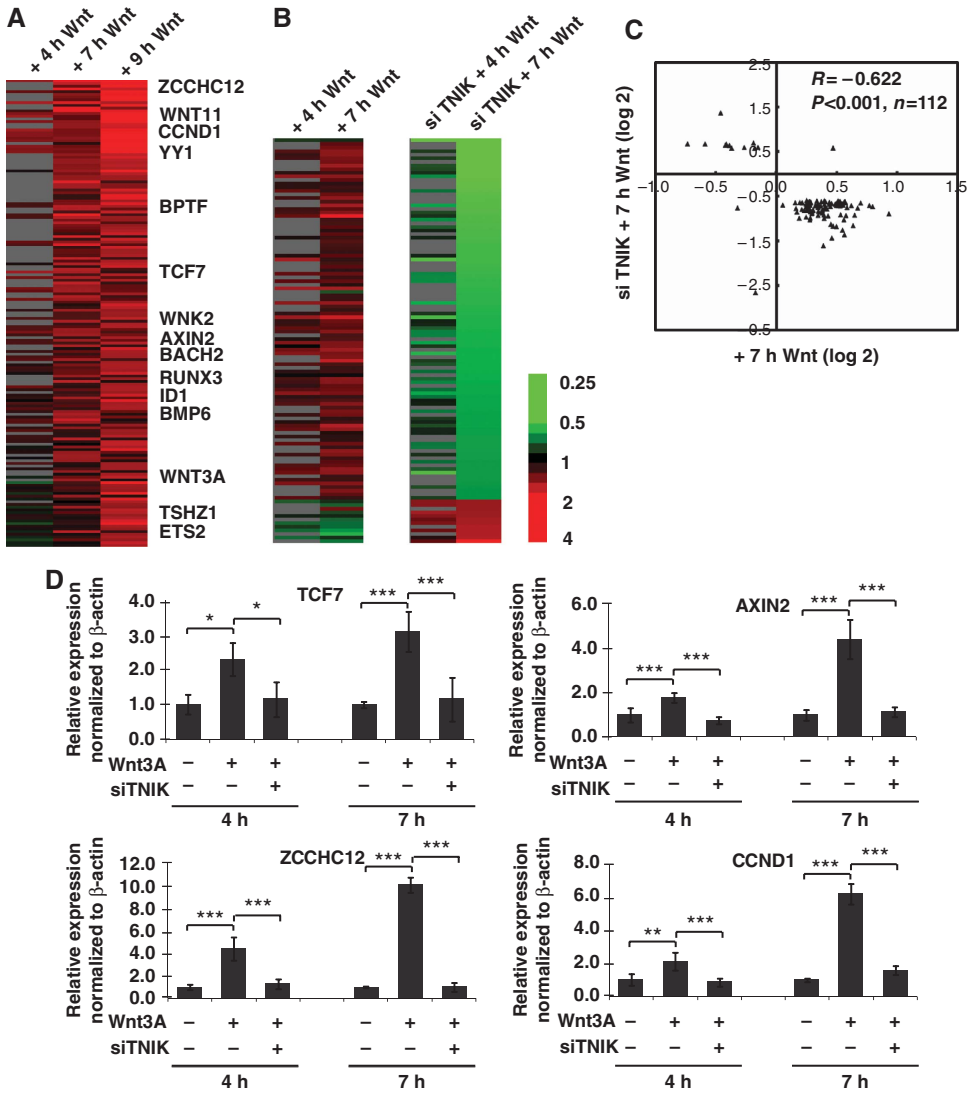

Figure 6 TNIK is an essential activator and specifically regulates Wnt target genes in HEK293T cells. (**A**) Expression pattern of 172 Wnt-induced genes selected against overlapping probes with 1.5-fold change in either 7 or 9 h Wnt induction. Representative Wnt-induced genes were listed. (**B**) Differential expression pattern of genes after TNIK suppression in HEK293T cells on 4 and 7 h Wnt induction with >1.5-fold variation at 7 h time point. The corresponding expression pattern on Wnt induction without TNIK suppression is shown on the left. Green, down-regulated after TNIK suppression; red, up-regulated after TNIK suppression; grey, missing data. (**C**) Significant negative correlation of the overlapping probes between 7 h WNT induction and TNIK suppression selected by 1.5-fold change after TNIK suppression. *x* axis: fold change (log2) after 7 h Wnt induction; *y* axis: fold change (log2) after TNIK suppression. (**D**) qRT–PCR validation of four selected candidate genes. **P*-value<0.05, ***P*-value<0.01, ****P*-value<0.001.

7 h time points (Supplementary Figure S3A). The negative association between the overlapping genes of 7 h Wnt induction in the presence or absence of TNIK (+7 h Wnt and si TNIK +7 h Wnt) was statistically significant (Pearson correlation coefficient, −0.508; $P<0.001$; Supplementary Figure S3B), in which genes up-regulated on Wnt induction were down-regulated after TNIK suppression and vice versa. These results suggest an essential function for TNIK in the regulation of Wnt target gene expression.

To understand whether TNIK is essential to Wnt pathway regulation, we filtered out 315 probes, representing 304 unique genes (Supplementary Table S2; Figure 6B) with 1.5-fold variation in Wnt-induced TNIK-depleted cells (si TNIK +7 h Wnt). Surprisingly, 91.4% (288 out of 315) of the probes were down-regulated at 7 h post Wnt induction on TNIK depletion, showing that TNIK serves preferentially as an activator in the Wnt-signalling pathway. In addition, 98% of the observed overlapping genes down-regulated on TNIK depletion were up-regulated after 7 h Wnt induction (Pearson correlation coefficient, −0.622; $P<0.001$; Figure 6C) indicating that TNIK is an essential component in the Wnt-signalling pathway. The results were reproduced by independent biological replicates with good correlation (Pearson correlation coefficient, 0.654; $P<0.001$; Supplementary Figure S4). To validate the microarray data, we chose four representative genes, *AXIN2*, *TCF7*, *CCND1* and *ZCCHC12* for quantitative RT–PCR (qRT–PCR) validation. All the selected genes were up-regulated in response to Wnt stimulation at 4 and 7 h. Expression of selected target genes was abrogated to basal levels on TNIK depletion, highlighting the essential function played by TNIK in activation of Wnt target genes (Figure 6D). In summary, our data show that TNIK serves as

an essential, specific activator in regulating the Wnt target gene signature.

Nuclear Wnt signalling requires the concerted action of numerous co-activating transcriptional complexes, many of which are enzymes such as CBP (Takemaru and Moon, 2000), p300 (Hecht *et al*, 2000) and MLL (Sierra *et al*, 2006; Mosimann *et al*, 2009). However, most of the co-activating enzymes implicated in TCF gene activation are pleiotropic factors involved in additional cellular processes and transcriptional pathways, and thus are not specific to regulation of Wnt signalling. In fact, despite the passage of a decade after the discovery of TCF4 and β-catenin as the molecular effectors of the Wnt signal, few transcriptional activators unique to Wnt transcriptional regulation have been found. Here, we report the identification of TNIK, a member of the STE20 GCK family (Fu *et al*, 1999), as a TCF4-interacting protein in the crypt-proliferative compartment of the mouse small intestine as well as in human colorectal cancer cells. TNIK is specifically recruited in a β-catenin-dependent manner to the Wnt target genes Axin2 and c-Myc. Expression of dominant negative TNIK kinase mutants abrogate TCF/LEF-reporter activity, highlighting the essential function of TNIK kinase activity in TCF4/β-catenin transcription regulation. Distinct regions of TNIK directly contact TCF4 and β-catenin and TNIK specifically phosphorylates TCF4. Examination of the function of TNIK by siRNA-mediated knockdown followed by gene expression array analysis identifies TNIK as an essential and specific co-activator of the Wnt target gene transcription programme, as over 90% of genes down-regulated in response to TNIK depletion were Wnt target genes.

Mammalian TNIK has three close homologues: NCK-interacting kinase (NIK)/MAP4K4, misshapen/NIK-related kinase (MINK) and NIK-related kinase (NRK). Although not conserved within the intermediate region, these NIK family members all share very high homology within the conserved N-terminal catalytic kinase domain as well as the C-terminal regulatory domain. In this study, our MS data specifically identified TNIK, and not the other homologous NIK family members, as a TCF4 interactor in the proliferative mouse intestinal crypt. The specific TNIK–TCF4 interaction despite the expression of both MINK and NIK in the crypt compartment (Vries RG *et al*, unpublished expression array data) is suggestive of a unique function for TNIK in regulating the Wnt-signalling pathway. Our current data reveals that TNIK binds to β-catenin through the unconserved intermediate domain, postulating that TNIK regulates the Wnt pathway by interacting with β-catenin, resulting in phosphorylation of TCF4 and transcription activation. The specificity of TNIK for the Wnt pathway, therefore, likely lies in the intermediate region, which is not conserved among the different NIK family members. Further study of the homologues on the binding and phosphorlyation of β-catenin and TCF4 will help to clarify the mechanism of control of TCF/LEF/β-catenin transcription regulation. Given the interaction with β-catenin, it will also be of interest to determine whether TNIK regulates the activities of other TCF/LEF members in complex with β-catenin.

Subsequent study to probe the function for TNIK in the multitude of biological phenomena controlled by Wnt signalling will be important. The current data imply TNIK as a potential target for the generation of small molecule inhibitors to specifically block the Wnt pathway in disease states such as colorectal cancer.

Materials and methods

Biochemical fractionation of mouse crypt and villus

The small intestine of four 6–12-week-old BALB C mice killed by CO2 chambers and cervical dislocation was removed, flushed with ice-cold PBS and cut open longitudinally to expose crypts and villi. Small intestine was cut into small 1–2 cm pieces and crypt and villus fractions were isolated using incubations in a mild PBS–EDTA/EGTA chelation solution combined with vigorous shaking followed by further purification using 70 μm (for villi) and 40 μm (for crypts) nylon cell strainer (Falcoln). Briefly, intestine pieces were washed several times in cold $PBS^{+/+}$ (Ca^{++}/Mg^{++}) and incubated in PBS^{0}EDTA–EGTA (no Ca^{++}/Mg^{++} + 1 mM EDTA + 1 mM EGTA) 10 min on rotator. Buffer was decanted followed by addition of fresh PBS^{0} and vigorous shaking approximately 10–15 times. Incubation in PBS^{0}EDTA–EGTA, decanting and shaking in PBS^{0} was repeated. Fractions were put through a 70-μm strainer. Whole villus structures remain on top of cell strainer and are collected, whereas the flow through (F/T) discarded. Incubation, shaking and separation through cell strainer was repeated and fractions 2–5 collected containing pure villus structures. From fraction 5, the F/T of the cell strainer containing intact crypts was collected and further purified by passage through a 40-μm cell strainer. This was repeated until the mesenchyme was stripped of epithelial cells. Typically, fractions 2–4 contained pure villi, whereas fractions 6–8 F/T contained pure crypts. Purified crypts and villi were washed twice and kept in $PBS^{+/+}$ for up to 1 h before further use.

DNA constructs

Details of cloning procedures are available on request. Briefly, using a PCR-based strategy, a sequence encoding the FLAG epitope was added at the beginning of the TCF4, β-catenin and TNIK-coding sequences and cloned into pcDNA3.1 (Invitrogen). For expression of GST-fusion proteins, the coding sequences of TCF4 and β-catenin were cloned in pGEX6P-1. For *in vitro* transcription/translation of TNIK deletions, indicated regions of TNIK-coding sequence were cloned in pcDNA3.1 (Invitrogen).

Immunoprecipitation

Total cellular extracts from Ls174T cells, HEK293T cells or primary mouse crypt or villus material were prepared in PLB buffer (1% Triton X-100, 2 mM EDTA, 1 mM DTT, 5% glycerol in PBS) supplemented with protease inhibitors (PIs) (Complete, Roche Molecular Biochemicals). Cellular lysates were pre-cleared with IgG-agarose beads (Sigma) for 6 h at 4°C. IPs of endogenous complexes from mouse crypt and villus, Ls174T and HEK293T cells were carried out overnight at 4°C with anti-TCF4 (Santa Cruz), anti β-catenin (BD transductions) or anti-TNIK (Santa Cruz) (2 μg/ml) in combination with a 50% protein G-Agarose slurry (Sigma). Immunoprecipitated material was washed three times in PLB supplemented with PIs. Bound proteins were subjected to SDS–PAGE and western blot analysis or mass spectrometry analysis.

MS analysis

In-gel digestion. Gel bands putatively containing TCF4, β-catenin and TNIK were sliced out from the gels of all four pull downs (i.e. αIgG villus, αTCF4 villus, αIgG crypt, αTCF4 cryo), Figure 1B, and subjected to in-gel digestion as described earlier (Shevchenko *et al*, 1996). Protein reduction and alkylation was performed with DTT (60°C, 1 h) and iodoacetamide (dark, RT, 30 min), respectively. Digestion was performed with trypsin over night at 37°C. Peptides were extracted with 10% FA.

NanoLC–MS/MS. The extracted peptides were subjected to nanoscale liquid chromatography tandem MS (nanoLC–MS/MS) analysis, performed on an Agilent 1100 HPLC system (Agilent technologies) connected to an LTQ Linear Ion Trap Mass Spectrometer combined with either an Orbitrap (ThermoFisher, Waltham, MA, USA) or a Fourier Transform Ion Cyclotron Resonance cell (ThermoFisher, Waltham, MA, USA). The nanoLC was equipped with a 20 mm × 100 μm i.d. Aqua C18 trap column (Phenomenex,

Torrance, CA, USA) and a 400 mm × 50 μm i.d. Reprosil C18 analytical column (Dr Maisch, Ammerbuch-Entringen, Germany) (Pinkse *et al*, 2008). Trapping was performed at a flow of 5 μl/min for 10 min and the fractions were eluted using a 45-min linear gradient from 0 to 40% solvent B (0.1 M acetic acid in 80% ACN (v/v), in which solvent A was 0.1 M acetic acid), 40–100% solvent B for 2 min and 100% B for 2.5 min. The analytical flow rate was 100 nl/min and the column effluent was directly introduced into the ESI source of the MS using a standard coated fused silica emitter (New Objective, Woburn, MA, USA) (o.d. 360 μm, tip i.d. 10 μm) biased to 1.7 kV. The mass spectrometer was operated in positive ion mode and in data-dependent mode to automatically switch between MS and MSMS. The three most intense ions in the survey scan were fragmented in the linear ion trap using collisional-induced dissociation. The target ion setting was 5e5 for the Orbitrap, with a maximum fill time of 250 ms and 1e6 for the FTICR, with a maximum fill time of 250 ms. Fragment ion spectra were acquired in the LTQ with an AGC value of 3e4 and a max injection time of 500 ms.

Protein identification. Raw MS data were converted to peak lists using Bioworks Browser software, version 3.1.1. Spectra were searched against the International Protein Index (IPI) human database version 3.36 (69012 sequences; 29002682 residues) or against the IPI mouse database version 3.36 (51326 sequences; 23682061 residues) using Mascot software version 2.2.0 (www.matrixscience.com), with trypsin set as enzyme. The database search was made with the following parameters set to consider a peptide tolerance of ± 15 p.p.m., a fragment tolerance of ± 0.9 Da, allowing three missed cleavages, carbamidomethyl (C) as fixed modification and oxidation (M).

Immunohistochemistry

Tissues were fixed in 10% formalin, paraffin embedded and sectioned. Antibodies such as rabbit anti-Tnik (1:1000, Santa Cruz) and mouse anti-Tnik, and clone 3D4 (1:500, Abnova) were used. Peroxidase conjugated secondary antibodies used were mouse or rabbit EnVision+ (DAKO).

In vitro binding assay

^{35}S-labelled reticulocyte-expressed TNIK deletion mutants were generated using the TNT quick-coupled transcription translation kit (Promega). Bacterially expressed GST, GST–TCF4 and GST–β-catenin were immobilized and purified on Glutathione beads for 2 h at 4°C followed by extensive washes with HEMG buffer [25 mm HEPES-KOH (pH 7.6), 0.1 mm EDTA, 12.5 mm $MgCl_2$, 10% glycerol, 1 mm DTT, 0.01% Nonidet P-40 (NP-40), protease and phosphatase inhibitors] containing 0.5–0.1 M KCl. Beads were incubated for 2 h with ^{35}S-labelled reticulocyte-expressed TNIK deletion mutants, washed extensively with HEMG buffer containing 0.1 M KCl and analysed by SDS–PAGE followed by autoradiography.

In vitro kinase assay

Immunoprecipitated WT or mutant Flag-TNIK was incubated with purified GST–TCF4 and GST–β-catenin-fusion proteins. Phosphorylation reactions were performed in 30 μl kinase buffer (20 mM Hepes (pH 7.5), 20 mM $MgCl_2$, 0.1 mM orthovanadate, and 2 mM dithiothreitol) supplemented with 20 μM ATP and 5 μCi of [γ-^{32}P]ATP at 30°C for 30 min. Reactions were stopped by the addition of 4 × Laemmli sample buffer and resolved by SDS–PAGE followed by autoradiography.

RNA interference

Pre-designed Dharmacon siRNA pools targeting transcripts of the human TNIK(L-004542-00) and non-target control siRNA pool (D-001810-10-20) were used to knock down TNIK in Ls174T colorectal cancer and HEK293T cells. siRNA was delivered into Ls174T, SW480 and HEK 293T cells using the siLentFect Lipid Reagent (Bio-Rad). siRNA (15 nM) was used to transfect 2×10^5 cells, and protein levels were examined by western blot analysis 72 h after transfection.

Transient transfection and luciferase assays

Ls174T CRC and HEK 293T cells were seeded at a density of 2×10^5 cells/12-well plate. siRNA targeting the human TNIK gene or control non-targeting siRNA was delivered the next day with siLentFect Lipid Reagent (Bio-Rad) according to the manufacturer's instructions. After 72 h, cells were transfected with plasmid constructs pGL-TOP and pGL-FOP optimal and mutated TCF luciferase-reporter constructs as described earlier (van de Wetering *et al*, 2002). The cells were lysed after 24 h using luciferase lysis buffer (Promega Corp.), and luciferase activities were measured using the Dual-Luciferase-reporter assay system. Transfection efficiency was normalized using the cotransfected *Renilla* luciferase activity as an internal control. The data shown are of two independent triplicate experiments as the mean ± s.d. of the ratio between the TOP/FOP and *Renilla* reporters.

Chromatin immunoprecipitation

Ls174T CRC cells or purified mouse crypt and villus fractions were fixed by adding formaldehyde to a final concentration of 1% for 30 min at room temperature. Glycine was added to a final concentration of 125 mM to quench the reaction. Cells were washed twice with buffer B (0.25% Triton X-100, 1 mM EDTA, 0.5 mM EGTA, 20 mM Hepes, pH7.6) and buffer C (150 mM NaCl, 1 mM EDTA, 0.5 mM EGTA, 20 mM Hepes, pH 7.6). Cells were resuspended in 0.3% SDS, 1% Triton –X-100, 0.15 M NaCl, 1 mM EDTA, 0.5 mM EGTA, 20 mM Hepes, pH7.6) and sheared using a BioRuptor sonicator (Cosmo Bio Co., Ltd) with 12 30-s pulses at the maximum setting. A total of 5 μg of the indicated antibody TCF4 (Santa Cruz), β-catenin (BD transduction) and TNIK (Santa Cruz) was incubated with the sheared cross-linked chromatin and BSA blocked protein-G beads overnight at 4°C. Approximately 20 million cells were used per IP. IPs were washed twice with each buffer1 (0.1% SDS, 0.1% deoxycholate, 1% Triton X-100, 150 mM NaCl, 1 mM EDTA, 0.5 mM EGTA, 20 mM Hepes pH7.6), buffer2 (0.1% SDS, 0.1% deoxycholate, 1% Triton X-100, 0.5 M NaCl, 1 mM EDTA, 0.5 mM EGTA, 20 mM Hepes pH7.6), buffer3 (250 mM LiCl, 0.5% deoxycholate, 0.5% NP-40, 1 mM EDTA, 0.5 mM EGTA, 20 mM Hepes, pH7.6) and buffer4 (1 mM EDTA, 0.5 mM EGTA, 20 mM Hepes, pH7.6). Immunoprecipitated complexes were eluted in 1% SDS, 0.1 M $NaHCO_3$ for 20 min and incubated overnight at 65°C for removal of crosslinks in the presence of 200 mM NaCl. DNA was phenol:chloroform extracted, chloroform:isoamylalcohol extracted, ethanol precipitated. Input and immunoprecipitated DNA were subjected to Sybergreen qPCR with primers overlapping the promoters, upstream/downstream regulatory regions of mouse and human Axin2 and c-Myc genes.

Quantitative PCR

ChIP experiments were analysed by qPCR in an iCycler iQ real-time PCR detection system (Bio-Rad) using iQ Sybergreen Supermix (Bio-Rad). ChIP values were normalized as a percentage of input, and presented as fold enrichment over the percentage of input immunoprecipitated over the second exon of the myoglobin gene (human samples) and the Sp5 downstream region (mouse samples) as control. The following primer pairs were used for examining recruitment to the human Axin2 promoter: 5′-GTTACCTGGAAGACG AAGG-3′; 5′-TCTGGAGGCGTTCAGTTG-3′, human Axin2 upstream control region: 5′-GCCAGAGTCAAGCCAGTAGT-3′; 5′-TAGCCTAATG TGGAGTGGAT-3′, mouse Axin2 promoter: 5′-CCACCAAGACCTACA TAC-3′; 5′-CCACTCCTCACATATTCC-3′, mouse Axin2 downstream control region: 5′-CTACCGTGTTACTCTGACTATTCTTC-3′; 5′-GCGGC TCAGTGGCTAAGG-3′, human c-Myc promoter: 5′-ACTCAGTCTGGG TGGAAGG-3′; 5′-GGAATGATAGAGGCATAAGGAGTATC-3′, human c-Myc downstream control region: 5′-CAGCAAGATAGCAGAG GAAG-3′; 5′-TGGAGATGGATTGAATGAAGG-3′, mouse c-Myc promoter: 5′-CTCACTGGAACTTACAATCTG-3′; 5′-CAACGCCCAAAGGA AATC-3′, mouse c-Myc upstream control region: 5′-ACTCAAGAACT GGTAGAC-3′; 5′-CTAAGTGGGTAAGGTAGG-3′, second exon of human Myoglobin gene: 5′-AAGTTTGACAAGTTCAAGGACC-3′; 5′-TGGCACCATGCTTCTTTAAGTC-3′, mouse Sp5 downstream control region: 5′-TGGAGTTACAGGCAGTGGTG-3′; 5′-ATTGATTTCTTTAGG TTGGGTGGAG-3′.

Site-directed mutagenesis

TNIK kinase mutants TNIK R152A/D153A, TNIK K54A and TNIK D171A/F172A were generated using the Quick Change Site-Directed Mutagenesis kit (Stratagene). WT full-length flag-tagged TNIK expression vector was used as a template for PCR-based mutagenesis using the following primers: TNIK R152A/D153A for 5′-CCAG CATAAAGTGATTCATGCAGCTATTAAAGGGCAAAATGTCTTG-3′, TNIK R152A/D153A Rev 5′-CAAGACATTTTGCCCTTTAATAGCTGCATGA ATCACTTTATGCTGG-3′, TNIK K54A for 5′-GCCAGCTTGCAGCCATC GCGGTTATGGATGTCACAGG-3′, TNIK K54A Rev 5′-CCTGTGACATC

CATAACCGCGATGGCTGCAAGCTGGC-3′, TNIK D171A/F172A for 5′-GCAGAAGTTAAACTAGTGGCCGCTGGAGTCAGTGCTCAGC-3′, TNIK D171A/F172A Rev 5′-GCTGAGCACTGACTCCAGCGGCCACTAGTTTAACTTCTGC-3′.

Microarray analysis

Total RNA was extracted from HEK293T cells after siRNA transfection (siTNIK or siNon target control) and induced with Wnt3A expressing conditioned medium (Wnt3A) or control medium (CM) for 4, 7 or 9 h using RNeasy Mini Kit (Qiagen) according to ATCC instruction. A total of 2 μg of RNA from each sample was labelled by Quick Amp Labelling Kit, two colour (Agilent) and corresponding pairs of samples were hybridized to 4X44K whole human genome dual colour microarrays (Agilent, G4112F). Six pair of samples: si-control + Wnt3A 4 h/si-control + CM 4 h (+4 h Wnt); si-control + Wnt3A 7 h/si-control + CM 7 h (+7 h Wnt); si-control + Wnt3A 9 h/si-control + CM 9 h (+9 h Wnt); si-TNIK + Wnt3A 4 h/si-control + Wnt3A 4 h (siTNIK + 4 h Wnt); si-TNIK + Wnt3A 7 h/si-control + Wnt3A 7 h (siTNIK + 7 h Wnt, Experiment1); si-TNIK + Wnt3A 7 h/si-control + Wnt3A 7 h (siTNIK + 7 h Wnt, Experiment2) were hybridized in two dye swap experiments resulting in 12 individual arrays. Microarray signal and background information were retrieved using Feature Extraction programme (V.9.5.3, Agilent Technologies). For each pair of experiment, fluorescent signals in either channel with greater than two times above the local background and showing the same trend of fold change in the corresponding dye swap experiments were considered as well measured and average was taken. Overlapping genes with >1.5-fold variations in either +7 h Wnt or +9 h Wnt (144 unique genes) were selected as Wnt-regulated genes in HEK293T cells, whereas genes with >1.5-fold variation (304 unique genes) in siTNIK +7 h Wnt were selected as TNIK-regulated genes. Array data is available at Gene Expression Omnibus under accession number GSE17623.

Statistical analysis

Comparison of differences between TOPFlash activities or qRT–PCR expression was performed using two-tailed Student *t*-test (in which equal variance between groups was assumed). To examine the correlation of expression fold change in corresponding microarray experiments, Pearson correlation was performed, whereas R represent correlation coefficient and P-value < 0.05 was considered as significant.

Supplementary data

Supplementary data are available at *The EMBO Journal* Online (http://www.embojournal.org).

Acknowledgements

We thank J van Es and M van den Born for providing the mouse small intestines used in our experiments. We also thank H Begthel for the immunostainings and H Teunissen for technical support. T Mahmoudi is funded by the Marie Curie Incoming International Fellowship (MC IIF 221108). V Li is supported by the Croucher Foundation Fellowship. RGJ Vries was funded by the Marie Curie Outgoing International Fellowship (MOIF CT 2004 002682). This work was supported by grants from the Centre for Biomedical Genetics and the Cancer Consortium.

Conflict of interest

The authors declare that they have no conflict of interest.

References

Barker N, Hurlstone A, Musisi H, Miles A, Bienz M, Clevers H (2001) The chromatin remodelling factor Brg-1 interacts with beta-catenin to promote target gene activation. *EMBO J* **20:** 4935–4943

Behrens J, von Kries JP, Kuhl M, Bruhn L, Wedlich D, Grosschedl R, Birchmeier W (1996) Functional interaction of beta-catenin with the transcription factor LEF-1. *Nature* **382:** 638–642

Bienz M, Clevers H (2000) Linking colorectal cancer to Wnt signalling. *Cell* **103:** 311–320

Calnek D, Quaroni A (1993) Differential localization by *in situ* hybridization of distinct keratin mRNA species during intestinal epithelial cell development and differentiation. *Differentiation* **53:** 95–104

Clevers H (2006) Wnt/beta-catenin signalling in development and disease. *Cell* **127:** 469–480

Fu CA, Shen M, Huang BC, Lasaga J, Payan DG, Luo Y (1999) TNIK, a novel member of the germinal center kinase family that activates the c-Jun N-terminal kinase pathway and regulates the cytoskeleton. *J Biol Chem* **274:** 30729–30737

Hanks SK, Hunter T (1995) Protein kinases 6. The eukaryotic protein kinase superfamily: kinase (catalytic) domain structure and classification. *FASEB J* **9:** 576–596

Hatzis P, van der Flier LG, van Driel MA, Guryev V, Nielsen F, Denissov S, Nijman IJ, Koster J, Santo EE, Welboren W, Versteeg R, Cuppen E, van de Wetering M, Clevers H, Stunnenberg HG (2008) Genome-wide pattern of TCF7L2/TCF4 chromatin occupancy in colorectal cancer cells. *Mol Cell Biol* **28:** 2732–2744

He TC, Sparks AB, Rago C, Hermeking H, Zawel L, da Costa LT, Morin PJ, Vogelstein B, Kinzler KW (1998) Identification of c-MYC as a target of the APC pathway. *Science* **281:** 1509–1512

Hecht A, Vleminckx K, Stemmler MP, van Roy F, Kemler R (2000) The p300/CBP acetyltransferases function as transcriptional coactivators of beta-catenin in vertebrates. *EMBO J* **19:** 1839–1850

Jho EH, Zhang T, Domon C, Joo CK, Freund JN, Costantini F (2002) Wnt/beta-catenin/Tcf signalling induces the transcription of Axin2, a negative regulator of the signalling pathway. *Mol Cell Biol* **22:** 1172–1183

Korinek V, Barker N, Moerer P, van Donselaar E, Huls G, Peters PJ, Clevers H (1998) Depletion of epithelial stem-cell compartments in the small intestine of mice lacking Tcf-4. *Nat Genet* **19:** 379–383

Korinek V, Barker N, Morin PJ, van Wichen D, de Weger R, Kinzler KW, Vogelstein B, Clevers H (1997) Constitutive transcriptional activation by a beta-catenin-Tcf complex in APC−/− colon carcinoma. *Science* **275:** 1784–1787

Kramps T, Peter O, Brunner E, Nellen D, Froesch B, Chatterjee S, Murone M, Zullig S, Basler K (2002) Wnt/wingless signalling requires BCL9/legless-mediated recruitment of pygopus to the nuclear beta-catenin-TCF complex. *Cell* **109:** 47–60

Liu W, Dong X, Mai M, Seelan RS, Taniguchi K, Krishnadath KK, Halling KC, Cunningham JM, Boardman LA, Qian C, Christensen E, Schmidt SS, Roche PC, Smith DI, Thibodeau SN (2000) Mutations in AXIN2 cause colorectal cancer with defective mismatch repair by activating beta-catenin/TCF signalling. *Nat Genet* **26:** 146–147

Lustig B, Jerchow B, Sachs M, Weiler S, Pietsch T, Karsten U, van de Wetering M, Clevers H, Schlag PM, Birchmeier W, Behrens J (2002) Negative feedback loop of Wnt signalling through upregulation of conductin/axin2 in colorectal and liver tumours. *Mol Cell Biol* **22:** 1184–1193

Molenaar M, van de Wetering M, Oosterwegel M, Peterson-Maduro J, Godsave S, Korinek V, Roose J, Destree O, Clevers H (1996) XTcf-3 transcription factor mediates beta-catenin-induced axis formation in Xenopus embryos. *Cell* **86:** 391–399

Morin PJ, Sparks AB, Korinek V, Barker N, Clevers H, Vogelstein B, Kinzler KW (1997) Activation of beta-catenin-Tcf signalling in colon cancer by mutations in beta-catenin or APC. *Science* **275:** 1787–1790

Mosimann C, Hausmann G, Basler K (2009) Beta-catenin hits chromatin: regulation of Wnt target gene activation. *Nat Rev Mol Cell Biol* **10:** 276–286

Pinkse MW, Mohammed S, Gouw JW, van Breukelen B, Vos HR, Heck AJ (2008) Highly robust, automated, and sensitive online TiO2-based phosphoproteomics applied to study endogenous phosphorylation in Drosophila melanogaster. *J Proteome Res* **7:** 687–697

Roose J, Huls G, van Beest M, Moerer P, van der Horn K, Goldschmeding R, Logtenberg T, Clevers H (1999) Synergy between tumour suppressor APC and the beta-catenin-Tcf4 target Tcf1. *Science* **285:** 1923–1926

Rubinfeld B, Albert I, Porfiri E, Fiol C, Munemitsu S, Polakis P (1996) Binding of GSK3beta to the APC-beta-catenin complex and regulation of complex assembly. *Science* **272:** 1023–1026

Shevchenko A, Wilm M, Vorm O, Mann M (1996) Mass spectrometric sequencing of proteins silver-stained polyacrylamide gels. *Anal Chem* **68:** 850–858

Sierra J, Yoshida T, Joazeiro CA, Jones KA (2006) The APC tumour suppressor counteracts beta-catenin activation and H3K4 methylation at Wnt target genes. *Genes Dev* **20:** 586–600

Taira K, Umikawa M, Takei K, Myagmar BE, Shinzato M, Machida N, Uezato H, Nonaka S, Kariya K (2004) The Traf2- and Nck-interacting kinase as a putative effector of Rap2 to regulate actin cytoskeleton. *J Biol Chem* **279:** 49488–49496

Takemaru KI, Moon RT (2000) The transcriptional coactivator CBP interacts with beta-catenin to activate gene expression. *J Cell Biol* **149:** 249–254

Tetsu O, McCormick F (1999) Beta-catenin regulates expression of cyclin D1 in colon carcinoma cells. *Nature* **398:** 422–426

van de Wetering M, Oving I, Muncan V, Pon Fong MT, Brantjes H, van Leenen D, Holstege FC, Brummelkamp TR, Agami R, Clevers H (2003) Specific inhibition of gene expression using a stably integrated, inducible small-interfering-RNA vector. *EMBO Rep* **4:** 609–615

van de Wetering M, Sancho E, Verweij C, de Lau W, Oving I, Hurlstone A, van der Horn K, Batlle E, Coudreuse D, Haramis AP, Tjon-Pon-Fong M, Moerer P, van den Born M, Soete G, Pals S, Eilers M, Medema R, Clevers H (2002) The beta-catenin/TCF-4 complex imposes a crypt progenitor phenotype on colorectal cancer cells. *Cell* **111:** 241–250

Yan D, Wiesmann M, Rohan M, Chan V, Jefferson AB, Guo L, Sakamoto D, Caothien RH, Fuller JH, Reinhard C, Garcia PD, Randazzo FM, Escobedo J, Fantl WJ, Williams LT (2001) Elevated expression of axin2 and hnkd mRNA provides evidence that Wnt/beta-catenin signalling is activated in human colon tumours. *Proc Natl Acad Sci USA* **98:** 14973–14978

